Journal of Porous Materials
https://doi.org/10.1007/s10934-019-00763-5

Pd-KIT-6: synthesis of a novel three-dimensional mesoporous catalyst and studies on its enhanced catalytic applications

Suman Chirra[1] · Suresh Siliveri[1] · Ajay Kumar Adepu[1] · Srinath Goskula[1] · Sripal Reddy Gujjula[1] · Venkatathri Narayanan[1]

Abstract
Synthesis of a novel three-dimensional mesoporous Pd-KIT-6 is carried out by a room temperature sol–gel method. The synthesised material is well crystalline observed from the Small angle powder X-ray diffraction. Calcination at 550 °C for 8 h retains the structure. The particle sizes are in the micron range. Si/Pd ratio of the as-synthesized material is found to be 45 against the input ratio 100. Transmission electron micrograph reveals the presence of the porous hexagonal structure. Thermogravimetric studies reveal that the KIT-6 (Korea Advanced Institute of Science and Technology number 6) undergo less weight-loss compared to Pd-KIT-6, which indicates the material is more crystalline than its metal-free counterpart due to the enhanced crystallisation rate. These results also supported by BET-surface area and Transmission electron microscopic picture. The 960 cm^{-1} band at Fourier transform Infrared spectroscopic analysis shows that the incorporation of Pd in the framework. These FT-IR results also supported by Raman Spectroscopic analysis. Electron spin resonance spectroscopic analysis shows that the Palladium is present in the +2 oxidation state in as-synthesized samples. Diffused reflectance Ultraviolet–Visible spectroscopic results show that Palladium is in tetrahedral coordination. Microwave irradiated Suzuki–Miyaura (SM) cross-coupling reactions studied by using the Pd-KIT-6 catalyst in detail without any organic solvent at 100 °C for 10 min. The reaction carried out in the presence of phenyl iodide, phenylboronic ($PhB(OH)_2$), and K_2CO_3 produce biphenyl, with 98% yield. Change of halide to Phenyl bromide gave similar results, but Phenyl chloride gave lesser conversion (20%). It is due to the electronegativity difference between the halides. A plausible reaction mechanism is also proposed.

Keywords Three-dimensional · Mesoporous · Pd-KIT-6 · Catalytic activity

1 Introduction

In the last decade, Mesoporous materials have an important role in addressing some of the major problems facing society in the twenty-first century, such as energy storage, CO_2 sequestration, H_2 storage, therapeutics (for example, drug delivery) and catalysis [1]. The size of the pores and their distribution directly affect their ability to function in a particular application [2]. There has been an increasing interest in the design of ordered mesoporous transition materials have attracted considerable attention because of their fascinating unique properties such as high surface areas, uniform and well-defined pore size, narrow pore size distribution, geometries, compositions and selective adsorption ability, making them highly valuable model systems for various research areas, the 2D hexagonal (p6 mm) structures of mesoporous materials like MCM-41 (Mobil Composition of Matter-41) and SBA-15 (Santa Barbara Amorphous-15), have been invented and applied in the fields of adsorption, catalysis, drug delivery, separation, sensing, cosmetic applications and biological studies. KIT-6 (Korea Advanced Institute of Science and Technology-6) is a recently reported mesoporous silica with may be described by the gyroid infinite periodic minimal surface (IPMS) structure with cubic *Ia*3*d* symmetry with two interpenetrating bicontinuous mesopore system with tunable pore size. Both channel systems are interconnected by micropores. The interconnectivity can be tuned [3]. Among many kinds of mesoporous silica with different structures and porosities, KIT-6 was chosen as a typical example with relatively large pores. In contrast

✉ Venkatathri Narayanan
venkatathrin@yahoo.com

[1] Department of Chemistry, National Institute of Technology Warangal, Warangal, Telangana 506004, India

Published online: 28 May 2019

to materials with 2D hexagonal symmetry, the 3D cubic pore structure is highly branched and is highly accessible. KIT-6 has attracted the researchers by its promising applications in catalysis. KIT-6 have characteristic features like high thermal stability, higher surface area, tunable pores with pore walls and large pore volume. The increased diffusion rate of reactants and products during the reaction had achieved a greater dispersion of the catalyst [4–7].

Cross-coupling reactions catalysed by palladium metal have played an essential role in the field of organic synthesis [8–15]. The 2010 year Noble prize to this reaction in chemistry to signifies the importance of this field in science [16]. The first and foremost SM cross-coupling reaction using palladium as catalyst reported in the literature was between aryl halide (R-X) and aryl boronic acids, and this method is significant in the carbon–carbon bond development to be precise for the synthesis of unsymmetrical biaryls. It is essential because these biaryls are predominant components of pharmaceuticals [17]. They are also present in many herbicides, alkaloids and materials used in the field of engineering like liquid crystals, molecular wires and mostly conducting polymers, extensive use in the synthesis of useful organic compounds in agrochemistry, nucleoside analogues, natural products, pharmaceuticals and advanced materials [18–23]. The homogeneous catalysts are having higher turnover numbers and high activity. However, homogeneous catalysts cannot be separated easily from the reaction mixtures, and there is a problem of potentially expensive complexes which have to recycle. The product also may contain residual metal contaminations. Even though homogeneous catalysts possess many advantages, it is difficult to separate and recycle them [24]. As far as heterogeneous catalysts are concerned, they can overcome these problems [25–28]. Microwave irradiation is in global trend for eco-friendly synthesis in a green approach. When microwave irradiation used over the conventional methods, the reaction times have greatly minimised, and the product yields maximised [29, 30]. The most vital objective in the field of green chemistry was the disposal of the volatile organic solvents resulted in organic synthesis. The use of less energy uptake by the solvent-free organic reaction reduces the solvent wastes, which simplified the products.

In the present work, we have described the synthesis of Pd-KIT-6 catalyst by room-temperature sol–gel method and its characterisation by various advanced analytical techniques. The catalytic activity of Pd-KIT-6 in the presence of $PhB(OH)_2$, R-X (chlorides, bromides, and iodides), and K_2CO_3 under microwave irradiation (SM cross-coupling reaction) are studied. The catalytic performance of the resulting materials in the SM cross-coupling reaction of aryl halides with aryl boronic acids and the efficiency of recycling the resulting catalysts are reported herein.

2 Experimental

The typical synthesis procedure is as follows [31, 32] 6.00 g of Pluronic P123 and 10 mL of 37 wt% concentrated HCl solution dissolved in 217 mL of double distilled water. After dissolution, 7.39 mL of n-butanol was added to the above mixture and stirred for 1 h at room temperature. 12.9 g of Tetraethylorthosilicate and Palladium acetate (Si/Pd = 100) are added to the above homogenous solution, followed by stirring for 24 h at room temperature. The final gel molar ratio is SiO_2: 0.01 P123:1.38 BuOH: 5.05 HCl: 116.51 H_2O:0.13 Pd $(OAc)_2$. The solid particles are centrifuged, washed with double distilled water and methanol and dried at 100 °C for overnight. Finally, a portion of the sample is calcined at 550 °C in the tubular furnace for 5 h.

Powder X-ray diffraction pattern (XRD) analysis of the samples are carried out by using Rigaku Corporation X-ray diffractometer Ultima-IV, Japan using Ni-filtered Cu-K_a radiation source (l = 1.5406 °A) with a 2θ scan range of 0.7–80° at 40 kV and 30 mA. Morphology of the samples analyzed by TESCAN VEGA 3 LMU scanning electron microscope (SEM) operating at 10–20 kV. The pore width and size of the samples analyzed by JEOL JEM-2100 Transmission electron microscopy (TEM) instrument using an acceleration voltage of 200 kV. Thermo Gravimetry/Differential thermal analysis (TG/DTA) of the samples is carried out by Regulus NETZSCH, STA 2500, and Japan under an air flow at a heating rate of 10 °C/min. Nova-1000 Quantachrome used for the BET—surface area measurements of the catalyst by nitrogen adsorption/desorptions isotherms recorded at liquid nitrogen 77 K temperature. The Fourier transform infrared spectroscopic (FT-IR) studies of the materials recorded on a PerkinElmer 200 s FT-IR instrument at room temperature using KBr pellets in the range of 4000 to 400 cm^{-1}. Raman spectroscopic analysis is carried out on a Bruker senterra dispersive smaller scale Raman spectrometer (Bruker Optik GmbH, Ettingen, Germany outfitted with a confocal magnifying instrument, and liquid nitrogen cooled charge coupled identifier by utilising a laser source of wavelength 532 nm and recorded in the 50 to 1550 cm^{-1} spectral ranges). JEOL JES FA 100 (Japan) used for Electron spin resonance analysis. UV–Vis diffuse reflectance spectra of the samples recorded with $BaSO_4$ as the reference on Thermo Scientific Evolution 300 UV–Visible spectrophotometer. X-ray photoelectron spectroscopic (XPS) analysis was performed by using a Thermo Fisher Scientific Theta Probe Spectrometer (East Grinstead, UK) for elemental quantification.

The catalytic activity tested by the following method. A mixture of aryl iodide (1 mmol), $PhB(OH)_2$ (1.5 mmol) and K_2CO_3 (1.98 mmol) in a microwave reaction vial and

accumulation of 0.1 g of Pd-KIT-6 catalyst to the reaction mixture. The flask was planted to heat at the 100 °C with 360 W in a microwave reactor (LG) for 10 min. After cooling the reaction mixture to room temperature, the products analysed by Thin layer chromatography. When the reaction completed, distilled water (5.0 mL) was added to the above mixture and extracted with ether (5.0 mL)—the organic level in dehydrated over $MgSO_4$ and concentrated in vacuum. The unrefined product was further purified by chromatography on a silica gel column to afford the pure product.

2.1 NMR spectral analysis for biphenyl compound

^{1}H NMR (400 MHz, DMSO-d_6, 25 °C, TMS): δ 7.59 (d, 4H), 7.43–7.39 (t, 4H), 7.33–7.30 (d, 2H) ppm; ^{13}C NMR (400 MHz, DMSO-d_6, 25 °C, TMS) δ = 141.2, 128.7, 128.6, 127.3, 127.2 ppm; Colourless solid; m.p. 68–70 °C.

3 Results and discussion

The powder low-angle XRD patterns of pure KIT-6 and Pd-KIT-6 samples are presented in Fig. 1. With the incorporation of Pd into the KIT-6 framework, the intensity of the peaks slightly decreases, and the peak positions are shifted to lower values due to the enhancement of the pore width [33]. The characteristic peaks of 211 and 200 plane correspond to the cubic structure of pure mesoporous KIT-6. XRD pattern of KIT-6 and Pd-KIT-6 show a single peak for amorphous silica in the wide-angle region. Of course, it is similar to the other reported data for mesoporous materials. We did not observe any peak for amorphous Palladium.

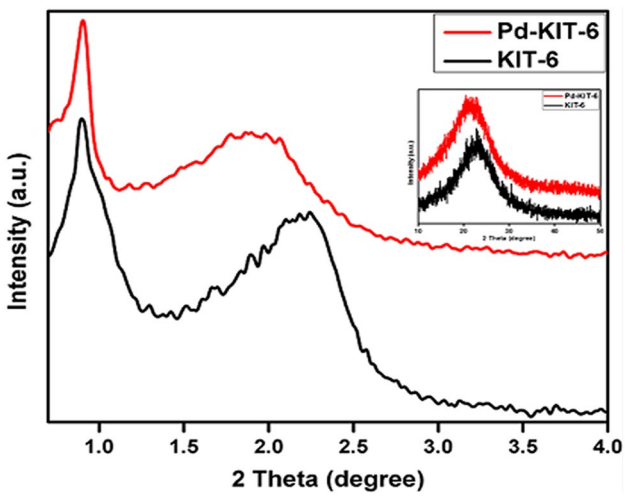

Fig. 1 Small angle and Wide angle (inset) XRD Pattern of KIT-6 and Pd-KIT-6

SEM pictures (Fig. 2) show the small cubic crystals of KIT-6 in the range of 10 µm, and there is no significant change in the morphologies of the crystals upon immobilisation of Pd particles [34]. The Energy dispersive X-ray analysis (EDAX) investigation results show that the presence of Si, O, C and Pd elements in the as-synthesized samples, the output Si/Pd = 45 against input Si/Pd = 100. The images show that there is an enrichment of Pd on the surface in the morphology of the synthesised material [35]. The palladium produces the active site in the material which improves the activity per site.

The morphology of KIT-6 and Pd- KIT-6 catalyst are investigated through TEM analysis, and the characteristic patterns displayed in Fig. 3. The Pd-KIT-6 was found to demonstrate an ordered three-dimensional hexagonal structure predictable with previous reports.

Thermogravimetric/Differential Thermal Analysis investigation was employed on as-synthesized KIT-6 and Pd-KIT-6 displayed in Fig. 4. In as synthesised KIT-6, there is an initial weight loss from 0 to 300 °C (9.7%) because of the desorption of physisorbed water. Another weight loss at 350 °C to 600 °C (30%) as a result of decomposition of template entrapped inside the pores of KIT-6 and in Pd-KIT-6 material there is an initial weight loss from 0 °C to 300 °C (2.7%) due to physisorption and chemisorption of water and another weight loss at 350 °C to 600 °C (60%) due to the oxidative decomposition of the template occluded in the pores of Pd-KIT-6. There is no weight loss of over 600 °C to 800 °C. KIT-6 and Pd/KIT-6 materials are thermally stable even up to 800 °C [36].

Nitrogen adsorption–desorption isotherms for the calcined KIT-6 and Pd-KIT-6 represented in Fig. 5. In general, for the uniform mesoporous KIT-6 material a clear capillary condensation step would be observed as it has been reflecting as its characteristic feature of the type-IV isotherm. The hysteresis loop H1 observed at a relatively high pressure which represents the distribution of channel-like pores and narrow pore size. Table 1 represents the textural properties of the surface area, pore volume and pore diameter of pure KIT-6 and Pd-KIT-6 respectively. A sharp decrease in the particular surface region of 974 m^2/g to 651 m^2/g. A slight decrease in the pore volume of 0.89 cc/g to 0.43 cc/g and there is no much change in the pore diameter. It confirms that there is a significant increase in crystallinity on Pd incorporation, probably due to enhancement in crystallisation rate [37].

Figure 6 provides information about FT-IR spectra of KIT-6 and Pd-KIT-6 catalyst. The band at 3449 cm^{-1} represents the –OH stretching vibration of water and defective -OH groups [38]. The resolved band at 1093 cm^{-1} relates to asymmetric stretching of Si–O–Si vibration. A band at 962 cm^{-1} is responsible for Si–O–H stretching vibration. The occurrence of bands at 1080, 802 and 464 cm^{-1} observed

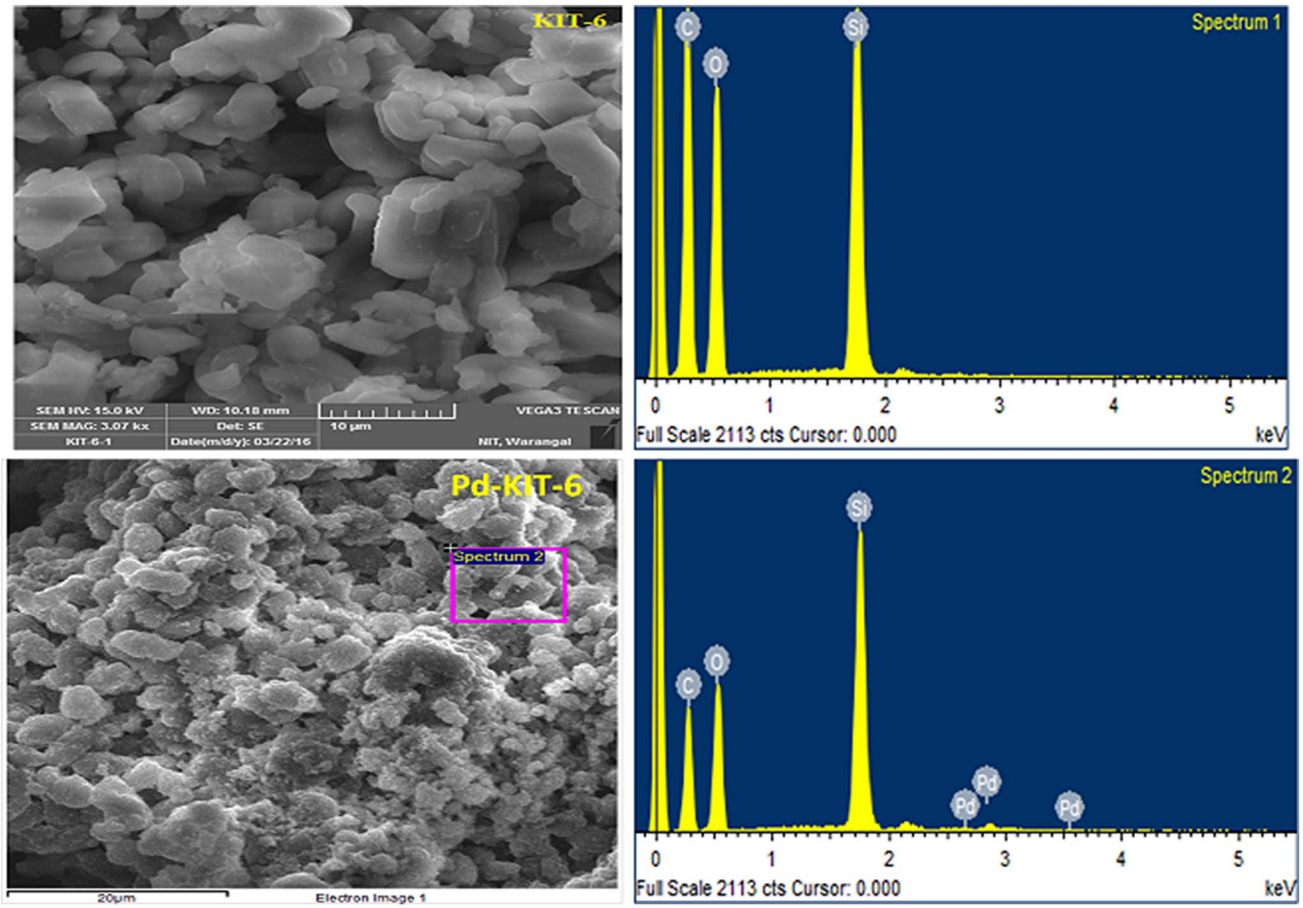

Fig. 2 Scanning electron micrograph and energy dispersive X-ray analysis of KIT-6 and Pd-KIT-6

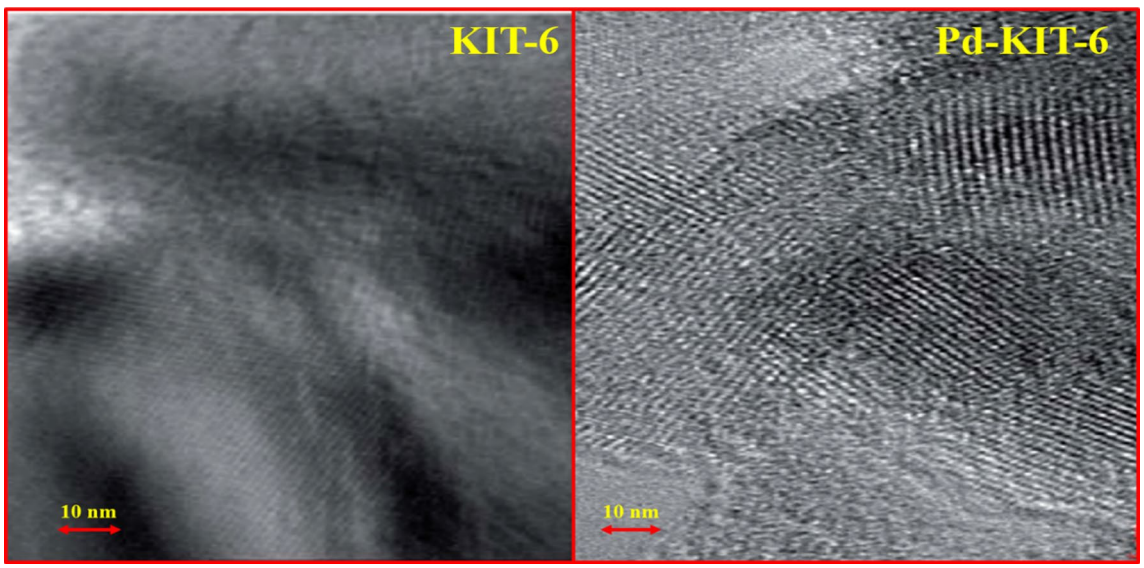

Fig. 3 Transmission electron micrograph of KIT-6 and Pd-KIT-6

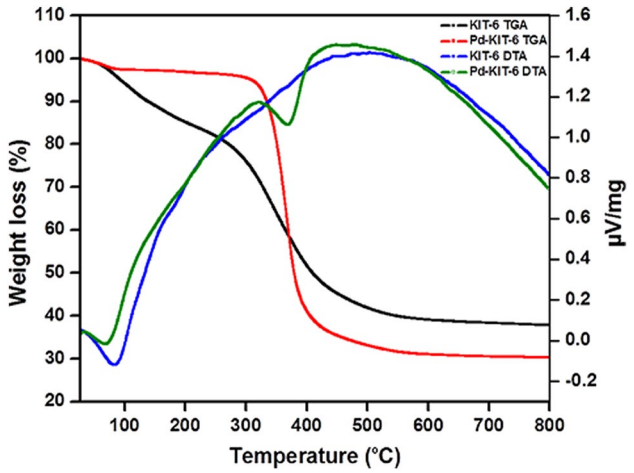

Fig. 4 Thermogravimetry/Differential thermal analysis of KIT-6 and Pd-KIT-6

due to the symmetric stretching and bending vibrations of Si–O–Si groups individually. 1644 cm^{-1} depicts the bending vibration of the water. The band present in Pd-KIT-6 at 2932 cm^{-1} is due to the presence of the template material.

The structural characteristic of Pd-KIT-6 catalyst was examined further with Raman spectroscopy. In Pd-KIT-6 the peak at 414 cm^{-1} relates to stretching vibration of Pd–O [39] (Fig. 7).

ESR spectrum of Pd-KIT-6 is shown in Fig. 8 It indicates typical hyperfine splitting of the presence of a broad background signal, and at field centre 327 (mT), g value is calculated as 2.004 which could be due to Pd^{2+}species present silica matrix.

The Ultraviolet–Visible Diffuse Reflectance Spectra (UV–Vis-DRS) of KIT-6 and Pd-KIT-6 analysed (Fig. 9) in the specific range of 200–800 nm. The characteristic absorption peak at 226 nm is due to the presence of Si–O^{-} species and the peak 380 nm is due to palladium present in tetrahedral coordination.

The oxidation state of Pd-KIT-6 was clearly observed in XPS analysis. Figure 10 show different peaks such as Pd, Si and O. A high intense peak around 532.8 eV was attributed to O1 s. The high-resolution XPS spectrum of the Pd 3d core level includes two components. Pd 3d 5/2 and Pd 3d 3/2 corresponds to the binding energy of 342 eV and 336 eV which is in agreement with the literature [40] displays the presence of Pd species in the material. The measured binding energy of 103.4 eV is assigned to Si 2p [41] Metal loading effect was clearly understood by XPS analysis. The deconvoluted spectrum of Pd metal was shown in inset Fig. 10. Presence of Pd^{2+} was clearly shown in the deconvoluted graph of Pd.

The calcined Pd-KIT-6 samples show a remarkable activity over the Suzuki–Miyaura reaction (Table 2). The reaction of $PhB(OH)_2$ with R-X accomplished by changing the nature

Table 1 BET surface area and porosity data

Mesoporous material	Pore volume[a] (cc/g)	Average pore diameter[b] (Å)	Surface area[c] (m^2/g)
KIT-6	0.89	36.62	974
Pd-KIT-6	0.43	36.61	651

[a]Pore volume evaluated from the N_2 adsorption–desorption isotherms

[b]Peak pore size determined from BJH pore size determination

[c]Surface area calculated using BET equation

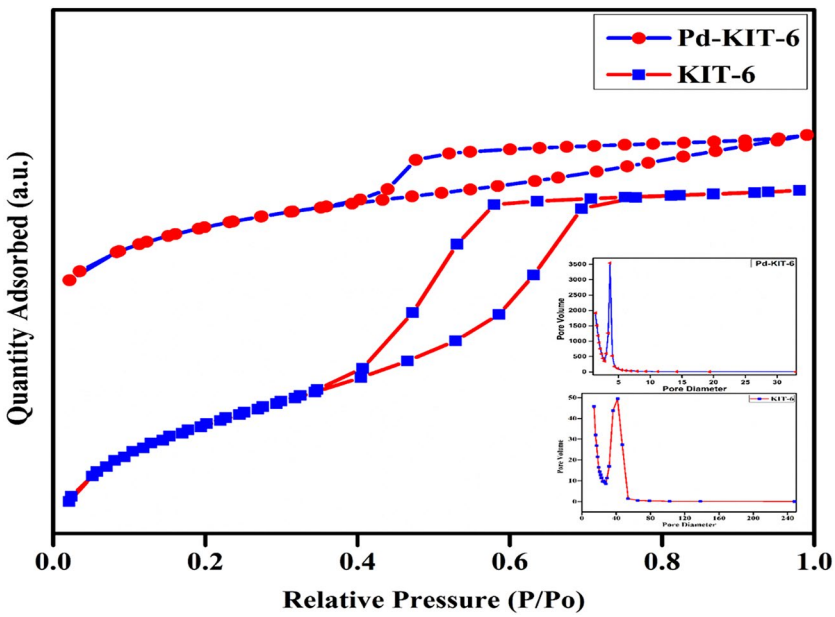

Fig. 5 N_2 Adsorption/Desorption isotherms and Pore diameter and Pore volume distributions of KIT-6 and Pd-KIT-6

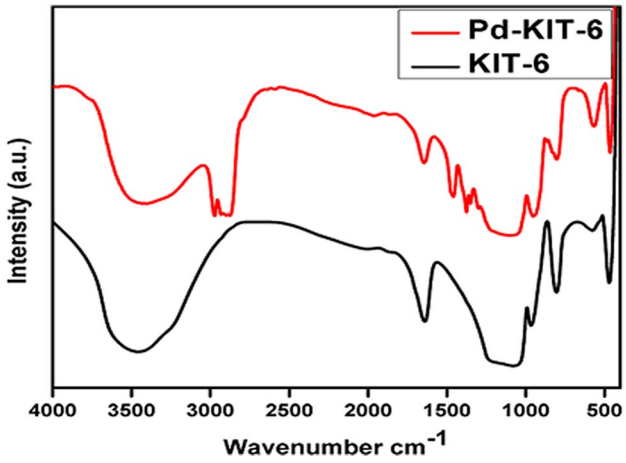

Fig. 6 FT-IR analysis of KIT-6 and Pd-KIT-6

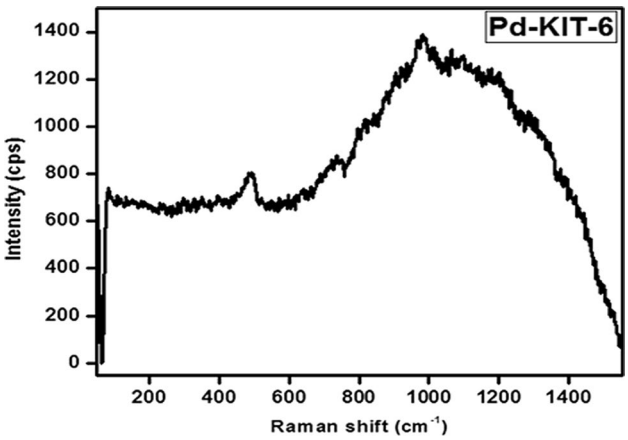

Fig. 7 Raman spectroscopy analysis of Pd-KIT-6

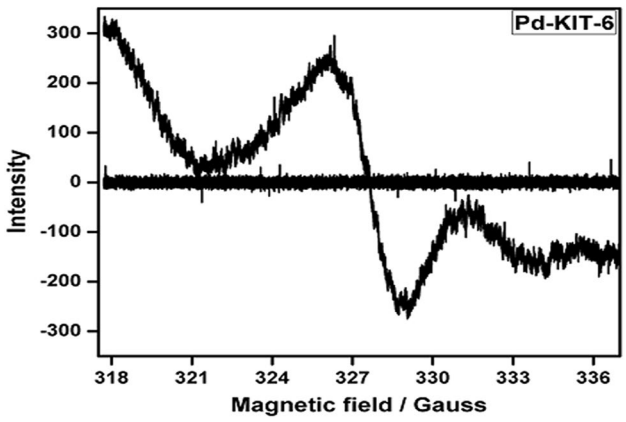

Fig. 8 Electron spin resonance analysis of as-synthesized Pd-KIT-6

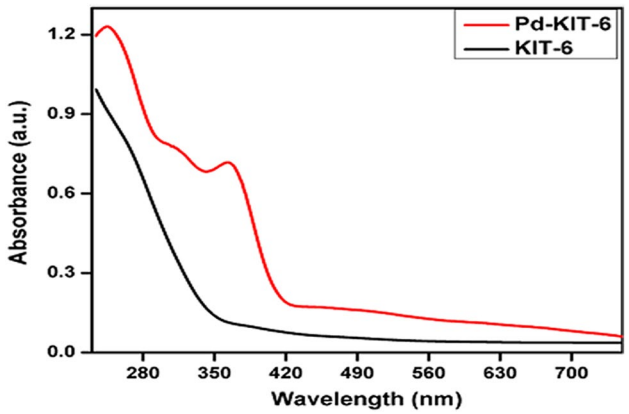

Fig. 9 Ultraviolet–Visible diffuse reflectance spectra of KIT-6 and Pd-KIT-6

of the substituent on the aryl halide. It is found that the reaction with aryl chloride occurred relatively slowly, taking at 10 min and yield only 20% of the product, whereas, for aryl bromide, the reaction took place in 10 min with 90% yield. The response with aryl iodide is found to be most efficient with 10 min of reaction time and yield 98%. Herewith the electronegativity of halides is assumed to play an important role.

The base is sophisticated in distinct steps of the catalytic cycle. It accelerates the rate of transmetalation between palladium and boron reagent. To find the most efficient base for the coupling reaction has been carried out in the occupancy of a series of bases like K_2CO_3, Na_2CO_3, Li_2CO_3, Cs_2CO_3, KF, K_3PO_4, KOH, and KO^{t}Bu (Table 3). In the attendance of K_3PO_4, KOH and KO^{t}Bu the yields were low, while Na_2CO_3, Li_2CO_3, Cs_2O_3, and KF gave moderate yields. The results show that the nature of the base much influences the cross-coupling reaction. Best results have observed in the presence of the K_2CO_3 base concerning both time and product yield, which was found to be 10 min and 98% respectively.

The reaction carried out by varying the changing of irradiation time for the sake of enhancing the reaction condition. When MW irradiation time shortened to 2 min at 100 °C with the maximum temperature at 300 W of power, the yield of the biphenyl diminished to 80%. It observed that the yield of biphenyl was declined to 92% and 84% when the irradiation time was raised to 20 and 30 min respectively. It emphasised that the best yield acquired from the following set of parameter MW irradiation at 100 °C, 300 W for 10 min with Pd-KIT-6 as a catalyst and K_2CO_3 used as a base (Table 4).

The reaction of aryl iodide with PhB $(OH)_2$ has analysed by varying the amount of catalyst. It observed that with an increase in the amount of catalyst from 0.02 to 0.10 g, a noticeable increment of 73 to 98% yield respectively (Table 5). Thus, the prescribed amount of 0.10 g was found to be the ideal for the composite with the contraction

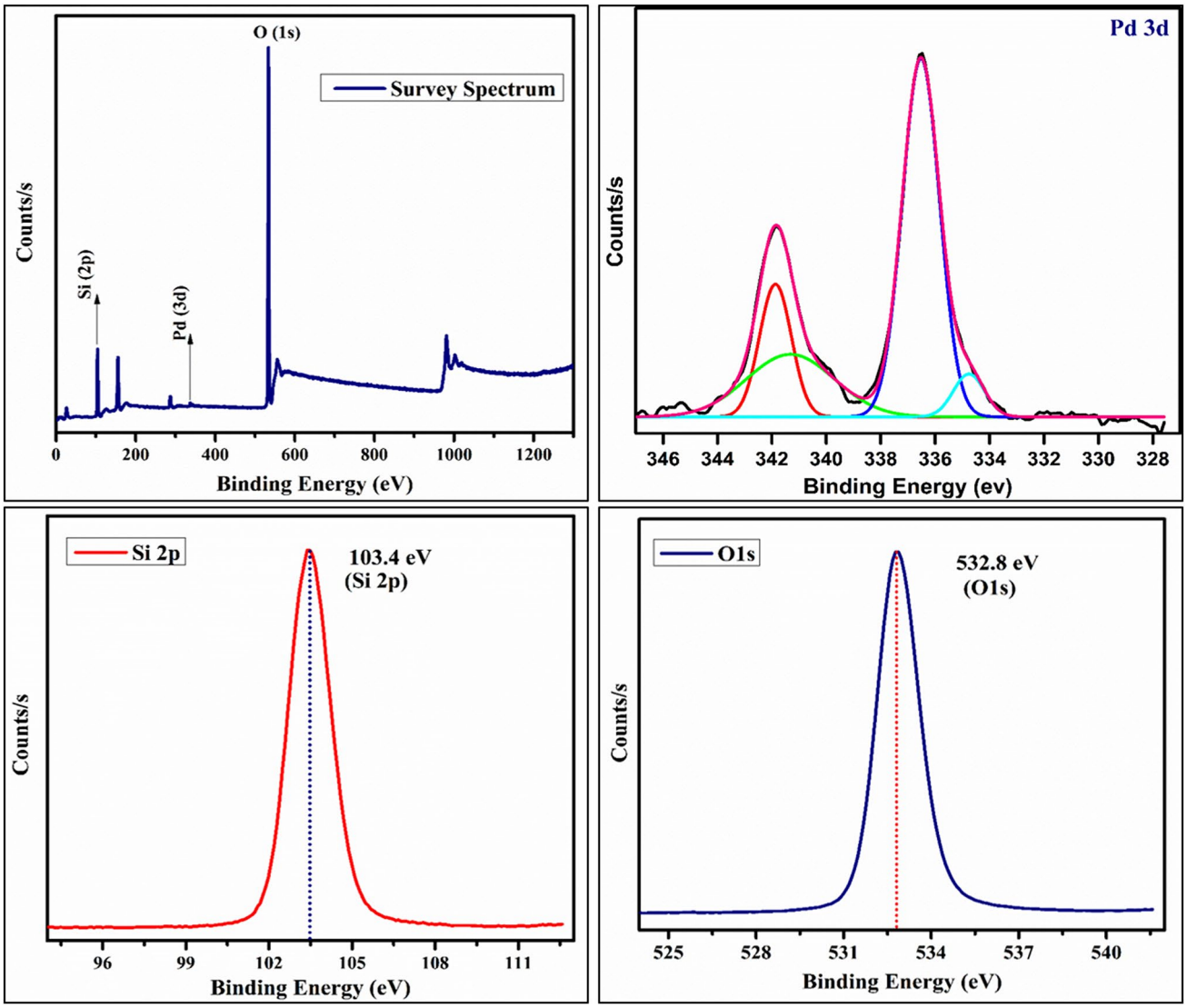

Fig. 10 XPS analysis of Pd-KIT-6

Table 2 Impact of substituents of R-Xs on SM cross-coupling reaction of $PhB(OH)_2$ with R-Xs (Reaction conditions: phenyl iodide (1 mmol), $PhB(OH)_2$ (1.5 mmol), base (1.98 mmol), Pd-KIT-6 (100 mg), 360 W, 100 °C)

S. No.	Aryl boronic acid	R-X	Base	Time (min)	Temp (°C)	Power (W)	Yield (%)
1	$PhB(OH)_2$	PhI	K_2CO_3	10	100	360	98
2	$PhB(OH)_2$	PhBr	K_2CO_3	10	100	360	90
3	$PhB(OH)_2$	PhCl	K_2CO_3	10	100	360	20

of PhB $(OH)_2$ (1.5 mmol) with iodobenzene (1 mmol) at 100 °C. It emphasised that in the absence of the catalyst there was no formation of products with the same reaction conditions. The reaction conditions are Aryl iodide (1 mmol), PhB $(OH)_2$ (1.5 mmol), Base (1.98 mmol), 360 W, 100 °C).

Feasibility of the catalyst further emphasised by multiple runs of the reaction on the same batch with the catalyst by the help of the model reaction. Then after the completion of the reaction process, the catalyst was recorded at the end of each cycle and reused by the filtration, washed with DDW 2–3 times, then with diethyl ether and acetone several times, the collected solid was dried in an oven at 60 °C for 12 h. It

Table 3 Result of bases in consideration of the M.W.-assisted SM cross-coupling reaction of $PhB(OH)_2$ and phenyl iodide with Pd-KIT-6 catalyst under solvent-free condition (Reaction conditions: Aryl iodide (1 mmol), $PhB(OH)_2$ (1.5 mmol), Base (1.98 mmol), Pd-KIT-6 dosage = 0.1 g)

S. No.	Base	Power (W)	Temperature (°C)	Time (min)	Yield (%)
1	K_2CO_3	360	100	10	98
2	Na_2CO_3	360	100	10	95
3	Li_2CO_3	360	100	10	86
4	Cs_2CO_3	360	100	10	82
5	KF	360	100	10	70
6	K_3PO_4	360	100	10	59
7	KOH	360	100	10	58
8	KO^{t}Bu	360	100	10	52

observed that after each run of the cycle the catalyst amount entirely recovered because of the filtration process. However, as per the recovered amount of the catalyst, the reactants precursors have been observed to run the next cycle. Despite being very less amount of catalyst lost during each run.

Further, we have tested the reusability of the Pd-KIT-6 catalyst with the reaction of the aryl iodide, and PhB $(OH)_2$ was carried out for two successive consecutive cycles by similar reaction conditions after the first reaction, the filtration process separated the solid product. The yields for the second and third cycles were found to be 97% and 95% respectively. For the fourth and fifth cycles were found to be 90% and 89% respectively. The catalyst has the capability with the outcome of the reusability for at least up to five cycles.

The SM cross-coupling reaction as shown in (Fig. 11) comes out of a three-step mechanism (i) oxidative addition (ii) transmetalation and (iii) reductive elimination [36]. In the oxidative addition process, palladium catalyst couples with the R-X which results in the formation of the organo-palladium complex. In the transmetalation step, the base activates the boron-containing in the reagent. The reaction does not at all take place in the absenteeism of the base. In the reductive elimination step, the essential product gained along with the regenerate of the palladium catalyst. The SM cross-coupling reaction was the organic reaction of an organoborane with an organohalide to produce the coupled product using a base and palladium-containing KIT-6 catalyst. The mechanism commences with the oxidative addition of the organohalide (R^1-X) to the Pd (II) complex. Organoborane to plan a borate reagent originating its R^2 group more nucleophilic than replaces the halide on the palladium complex. Transmetallation with the borate then follows where its R^2 group takes over from the halide anion on the palladium complex. Reductive elimination, at that moment hand over the final coupled product (Bi-phenyl compound), regenerates the palladium catalyst and the catalytic cycle be able to start over again.

4 Conclusions

The Pd-KIT-6 catalyst is synthesised by the room temperature sol–gel method, and various advanced techniques were used to characterise the materials. The synthesised materials are highly crystalline. The catalytic activity of this material is studied in the solvent-free condition under microwave radiation. We have optimised the reaction conditions and also a plausible mechanism on its catalytic activity is proposed.

Table 5 M.W.-assisted SM cross-coupling reaction of R-Xs with PhB $(OH)_2$ yield dependence of the catalyst amount (Reaction conditions: Aryl iodide (1 mmol), PhB $(OH)_2$ (1.5 mmol), Base (1.98 mmol), 360 W, 100 °C)

S.No.	Amount of catalyst (g)	Yield (%)
1	0	–
2	0.02	73
3	0.04	82
4	0.06	86
5	0.08	92
6	0.10	98

Table 4 MW-mediated SM cross-coupling reaction conditions: R-Xs with $PhB(OH)_2$ s and its reaction time

S. No.	Catalyst	Temperature (°C)	Power (W)	Base	Time (min)	Yield (%)
1	Pd-KIT-6	100	360	K_2CO_3	2	80
2	Pd-KIT-6	100	360	K_2CO_3	4	85
3	Pd-KIT-6	100	360	K_2CO_3	6	95
4	Pd-KIT-6	100	360	K_2CO_3	8	96
5	Pd-KIT-6	100	360	K_2CO_3	10	98
6	Pd-KIT-6	100	360	K_2CO_3	20	94
7	Pd-KIT-6	100	360	K_2CO_3	30	84

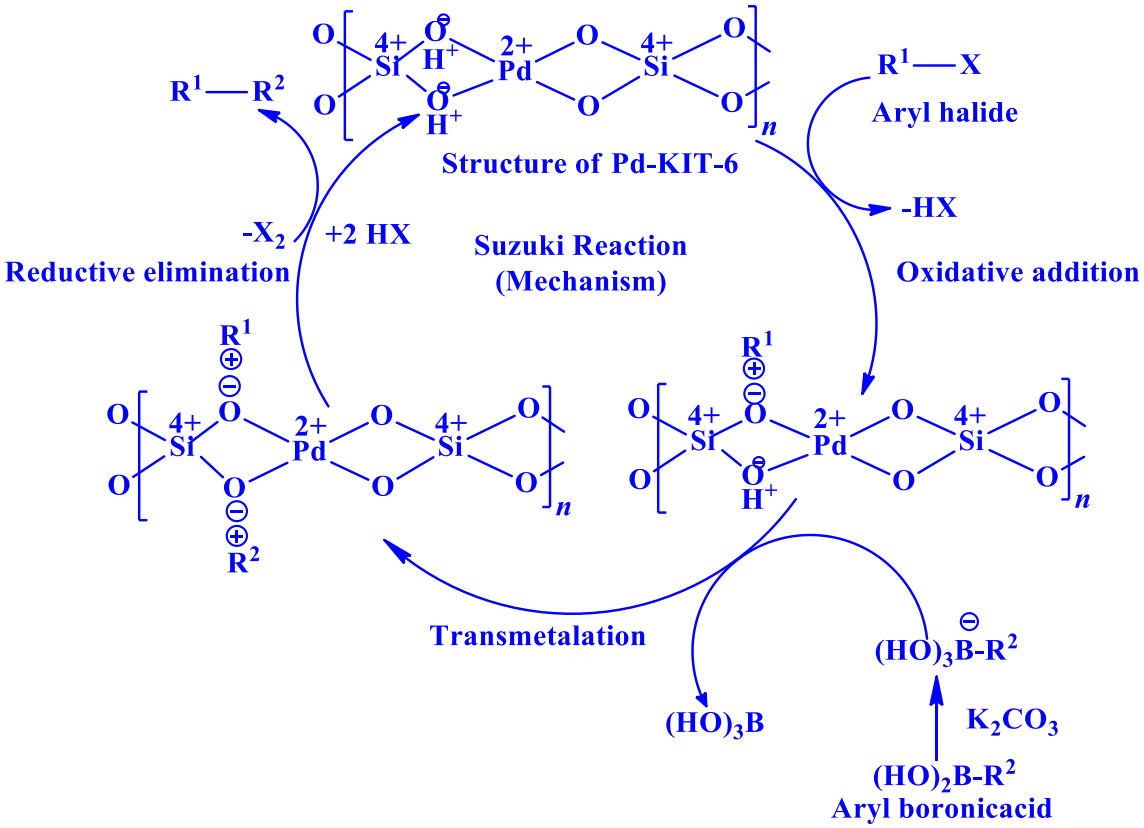

Fig. 11 A plausible reaction mechanism for SM cross-coupling reaction in the existence of Pd-KIT-6

Acknowledgements The authors thank MHRD, New Delhi for a research fellowship. We also thank DST-SERB (Research project Grant No. EMR/2014/000629), New Delhi for partial funding.

References

1. A. Corma, From microporous to mesoporous molecular sieve materials and their use in catalysis. Chem. Rev. **97**(6), 2373–2420 (1997). https://doi.org/10.1021/cr960406n
2. M.E. Davis, Ordered porous materials for emerging applications. Nature **417**(6891), 813–821 (2002). https://doi.org/10.1038/nature00785
3. T.-W. Kim, F. Kleitz, B. Paul, R. Ryoo, MCM-48-like large mesoporous silicas with tailored pore structure: facile synthesis domain in a ternary triblock copolymer–butanol–water system. J. Am. Chem. Soc. **127**(20), 7601–7610 (2005). https://doi.org/10.1021/ja042601m
4. J. Chen, J. Zhang, D. Zhu, T. Li, Novel polymer-supported phosphine palladium catalyst: one-pot synthesis from and application in Suzuki–Miyaura coupling reaction. J. Porous Mater. **24**(4), 847–853 (2016). https://doi.org/10.1007/s10934-016-0324-7
5. T. Tsoncheva, L. Ivanova, J. Rosenholm, M. Linden, Cobalt oxide species supported on SBA-15, KIT-5 and KIT-6 mesoporous silicas for ethyl acetate total oxidation. Appl. Catal. B **89**(3–4), 365–374 (2009). https://doi.org/10.1016/j.apcatb.2008.12.015
6. F. Zhang, Y. Zheng, Y. Cao, C. Chen, Y. Zhan, X. Lin, J. Zhu, Ordered mesoporous Ag–TiO2–KIT-6 heterostructure: synthesis, characterization and photocatalysis. J. Mater. Chem. **19**(18), 2771 (2009). https://doi.org/10.1039/b818495j
7. X. Liu, X. Zhao, M. Lu, Novel polymer supported iminopyridylphosphine palladium (II) complexes: an efficient catalyst for Suzuki-Miyaura and Heck cross-coupling reactions. J. Organomet. Chem. **768**, 23–27 (2014). https://doi.org/10.1016/j.jorganchem.2014.06.019
8. A. Modak, J. Mondal, V.K. Aswal, A. Bhaumik, A new periodic mesoporous organosilica containing diimine-phloroglucinol, Pd(II)-grafting and its excellent catalytic activity and trans-selectivity in C–C coupling reactions. J. Mater. Chem. **20**(37), 8099 (2010). https://doi.org/10.1039/c0jm01180k
9. J. Rathod, P. Sharma, P. Pandey, A.P. Singh, P. Kumar, Highly active recyclable SBA-15-EDTA-Pd catalyst for Mizoroki-Heck, Stille and Kumada C–C coupling reactions. J. Porous Mater. **24**(4), 837–846 (2016). https://doi.org/10.1007/s10934-016-0323-8
10. K. Dhara, K. Sarkar, D. Srimani, S.K. Saha, P. Chattopadhyay, A. Bhaumik, A new functionalized mesoporous matrix supported Pd(II)-Schiff base complex: an efficient catalyst for the Suzuki–Miyaura coupling reaction. Dalton Trans. **39**(28), 6395 (2010). https://doi.org/10.1039/c003142a
11. A. Pathak, A.P. Singh, Synthesis and characterization of D-2PA-Pd(II)@SBA-15 catalyst via "click chemistry": highly active catalyst for Suzuki coupling reactions. J. Porous Mater. **24**(2), 327–340 (2016). https://doi.org/10.1007/s10934-016-0266-0

12. N. Suzuki, S. Kiba, Y. Yamauchi, Fabrication of mesoporous silica KIT-6/polymer composite and its low thermal expansion property. Mater. Lett. **65**(3), 544–547 (2011). https://doi.org/10.1016/j.matlet.2010.10.027
13. Q. Liu, J. Li, Z. Zhao, M. Gao, L. Kong, J. Liu, Y. Wei, Synthesis, characterization, and catalytic performances of potassium-modified molybdenum-incorporated KIT-6 mesoporous silica catalysts for the selective oxidation of propane to acrolein. J. Catal. **344**, 38–52 (2016). https://doi.org/10.1016/j.jcat.2016.08.014
14. A. Gniewek, J. Ziolkowski, A. Trzeciak, M. Zawadzki, H. Grabowska, J. Wrzyszcz, Palladium nanoparticles supported on alumina-based oxides as heterogeneous catalysts of the Suzuki–Miyaura reaction. J. Catal. **254**(1), 121–130 (2008). https://doi.org/10.1016/j.jcat.2007.12.004
15. V.V. Namboodiri, R.S. Varma, Microwave-accelerated Suzuki cross-coupling reaction in polyethylene glycol (PEG). Green Chem. **3**(3), 146–148 (2001). https://doi.org/10.1039/b102337n
16. W. Chang, G. Chae, S.R. Jang, J. Shin, B.J. Ahn, An efficient microwave-assisted Suzuki reaction using Pd/MCM-41 and Pd/SBA-15 as catalysts in solvent-free condition. J. Ind. Eng. Chem. **18**(2), 581–585 (2012). https://doi.org/10.1016/j.jiec.2011.11.043
17. W. Chang, J. Shin, G. Chae, S.R. Jang, B.J. Ahn, Microwave-assisted Sonogashira cross-coupling reaction catalyzed by Pd-MCM-41 under solvent-free conditions. J. Ind. Eng. Chem. **19**(3), 739–743 (2013). https://doi.org/10.1016/j.jiec.2012.11.002
18. S. Liu, J. Xiao, Toward green catalytic synthesis—Transition metal-catalyzed reactions in non-conventional media. J. Mol. Catal. A: Chem. **270**(1–2), 1–43 (2007). https://doi.org/10.1016/j.molcata.2007.01.003
19. P. Das, D. Sharma, A.K. Shil, A. Kumari, Solid-supported palladium nano and microparticles: an efficient heterogeneous catalyst for ligand-free Suzuki–Miyaura cross coupling reaction. Tetrahedron Lett. **52**(11), 1176–1178 (2011). https://doi.org/10.1016/j.tetlet.2011.01.009
20. M. Bernechea, E. de Jesús, C. López-Mardomingo, P. Terreros, Dendrimer-Encapsulated Pd Nanoparticles versus palladium acetate as catalytic precursors in the stille reaction in water. Inorg. Chem. **48**(10), 4491–4496 (2009). https://doi.org/10.1021/ic9002753
21. V. Polshettiwar, C. Len, A. Fihri, Silica-supported palladium: sustainable catalysts for cross-coupling reactions. Coord. Chem. Rev. **253**(21–22), 2599–2626 (2009). https://doi.org/10.1016/j.ccr.2009.06.001
22. N. Noori, M. Nikoorazm, A. Ghorbani-Choghamarani, Pd(0)-S-methylisothiourea grafted onto mesoporous MCM-41 and its application as heterogeneous and reusable nanocatalyst for the Suzuki, Stille and Heck cross-coupling reactions. J. Porous Mater. **23**(6), 1467–1481 (2016). https://doi.org/10.1007/s10934-016-0207-y
23. T. Tamoradi, M. Ghadermazi, A. Ghorbani-Choghamarani, SBA-15@adenine–Pd: a novel and green heterogeneous nanocatalyst in Suzuki and Stille reactions and synthesis of sulfides. J. Porous Mater. **26**(1), 121–131 (2018). https://doi.org/10.1007/s10934-018-0623-2
24. R. Narayanan, M.A. El-Sayed, Effect of catalysis on the stability of metallic nanoparticles: suzuki reaction catalyzed by PVP-palladium nanoparticles. J. Am. Chem. Soc. **125**(27), 8340–8347 (2003). https://doi.org/10.1021/ja035044x
25. S. Kotha, K. Lahiri, D. Kashinath, Recent applications of the Suzuki–Miyaura cross-coupling reaction in organic synthesis. Tetrahedron **58**(48), 9633–9695 (2002). https://doi.org/10.1016/s0040-4020(02)01188-2
26. H. Filian, A. Ghorbani-Choghamarani, E. Tahanpesar, Pd(0)-guanidine@MCM-41 as efficient and reusable heterogeneous catalyst for C–C coupling reactions. J. Porous Mater. (2018). https://doi.org/10.1007/s10934-018-0698-9
27. K. Song, P. Liu, J. Wang, B. Tan, T. Li, Highly active palladium nanoparticles immobilized on knitting microporous organic polymers as efficient catalysts for Suzuki–Miyaura cross-coupling reaction. J. Porous Mater. **23**(3), 725–731 (2016). https://doi.org/10.1007/s10934-016-0127-x
28. A. Loupy, L. Perreux, M. Liagre, K. Burle, M. Moneuse, Reactivity and selectivity under microwaves in organic chemistry. Relation with medium effects and reaction mechanisms. Pure Appl. Chem. **73**(1), 161 (2001). https://doi.org/10.1351/pac200173010161
29. N.J.S. Costa, P.K. Kiyohara, A.L. Monteiro, Y. Coppel, K. Philippot, L.M. Rossi, A single-step procedure for the preparation of palladium nanoparticles and phosphine-functionalized support as a catalyst for Suzuki cross-coupling reactions. J. Catal. **276**(2), 382–389 (2010). https://doi.org/10.1016/j.jcat.2010.09.028
30. S. Suresh, I.A.K. Reddy, N. Venkatathri, Synthesis of SAPO-16 molecular sieve in the non-aqueous medium by microwave method using Hexamethyleneimine as a template. Microporous Mesoporous Mater. **263**, 275–281 (2018). https://doi.org/10.1016/j.micromeso.2017.12.008
31. X. Zhang, P. Zhang, H. Yu, Z. Ma, S. Zhou, Mesoporous KIT-6 supported Pd–M x O y (M=Ni Co, Fe) catalysts with enhanced selectivity for p-chloronitrobenzene hydrogenation. Catal. Lett. **145**(3), 784–793 (2015). https://doi.org/10.1007/s10562-015-1480-0
32. C. He, J. Li, X. Zhang, L. Yin, J. Chen, S. Gao, Highly active Pd-based catalysts with hierarchical pore structure for toluene oxidation: catalyst property and reaction determining factor. Chem. Eng. J. **180**, 46–56 (2012). https://doi.org/10.1016/j.cej.2011.10.099
33. M. Hussain, F.A. Deorsola, N. Russo, D. Fino, R. Pirone, Abatement of CH4 emitted by CNG vehicles using Pd-SBA-15 and Pd-KIT-6 catalysts. Fuel **149**, 2–7 (2015). https://doi.org/10.1016/j.fuel.2014.12.024
34. A.R. Siamaki, A.E.R.S. Khder, V. Abdelsayed, M.S. El-Shall, B.F. Gupton, Microwave-assisted synthesis of palladium nanoparticles supported on graphene: a highly active and recyclable catalyst for carbon–carbon cross-coupling reactions. J. Catal. **279**(1), 1–11 (2011). https://doi.org/10.1016/j.jcat.2010.12.003
35. R.J. Kalbasi, N. Mosaddegh, Palladium nanoparticles supported on Poly(2-hydroxyethyl methacrylate)/KIT-6 composite as an efficient and reusable catalyst for Suzuki-Miyaura reaction in water. J. Inorg. Organomet. Polym Mater. **22**(2), 404–414 (2011). https://doi.org/10.1007/s10904-011-9569-4
36. K. Soni, B.S. Rana, A.K. Sinha, A. Bhaumik, M. Nandi, M. Kumar, G.M. Dhar, 3-D ordered mesoporous KIT-6 support for effective hydrodesulfurization catalysts. Appl. Catal. B **90**(1–2), 55–63 (2009). https://doi.org/10.1016/j.apcatb.2009.02.010
37. J. Sun, Q. Kan, Z. Li, G. Yu, H. Liu, X. Yang, J. Guan, Different transition metal (Fe^{2+}, Co^{2+}, Ni^{2+}, Cu^{2+}or VO^{2+}) Schiff complexes immobilized onto three-dimensional mesoporous silica KIT-6 for the epoxidation of styrene. RSC Adv. **4**(5), 2310–2317 (2014). https://doi.org/10.1039/c3ra45599h
38. X. Wang, Y. Tseng, J. Chan, S. Cheng, Catalytic applications of aminopropylated mesoporous silica prepared by a template-free route in flavanones synthesis. J. Catal. **233**(2), 266–275 (2005). https://doi.org/10.1016/j.jcat.2005.04.007
39. A. Rajini, A.K. Adepu, S. Chirra, N. Venkatathri, Porous palladium aminophosphates: synthesis, characterization, antimicrobial and cytotoxicity studies. RSC Adv. **5**(82), 66956–66964 (2015). https://doi.org/10.1039/c5ra11923e

40. P.O. Thevenin, E. Pocoroba, L.J. Pettersson, H. Karhu, I.J. Väyrynen, S.G. Järås, Characterization and activity of supported palladium combustion catalysts. J. Catal. **207**(1), 139–149 (2002). https://doi.org/10.1006/jcat.2002.3515
41. L. Guo, J. Bai, C. Li, H. Liang, W. Sun, Q. Meng, T. Xu, Fabrication of palladium nanoparticles-loaded carbon nanofibers catalyst for the Heck reaction. New J. Chem. **37**(12), 4037 (2013). https://doi.org/10.1039/c3nj00609c